ISSN 0036-0244, Russian Journal of Physical Chemistry A, 2021, Vol. 95, No. 1, pp. 139–153. © Pleiades Publishing, Ltd., 2021.

STRUCTURE OF MATTER AND QUANTUM CHEMISTRY

New Syntheses of 4NPMA Homopolymer and Its Copolymer with Limonene: Experimental Analysis and Density Functional Theory Study

Nevin Çankaya[a,*], Emine Taniş[b], and Pembe Gül Sapan[a]

[a] *Department of Chemistry, Faculty of Science, University of Usak, Usak, Turkey*

[b] *Department of Electrical and Electronics Engineering, Kırşehir Ahi Evran University, Kırsehir, Turkey*

**e-mail: nevin.cankaya@usak.edu.tr; nevincankaya@hotmail.com*

Received October 9, 2019; revised October 9, 2019; accepted November 12, 2019

Abstract—The *N*-(4-nitrophenyl)methacrylamide homopolymer (poly(4NPMA)) and copolymer of limonene with *N*-(4-nitrophenyl)methacrylamide (4NPMA-co-LIM) have been synthesized and characterized by FT-IR and NMR spectroscopic methods. The spectroscopic properties of poly(4NPMA) and 4NPMA-co-LIM were predicted using Density Functional Theory (DFT) calculations. The results have been compared with observed values, and they match with each other. Frontier orbital analysis (FMOs), global reactivity descriptors, MEP as well as Mulliken atomic charge were calculated with same method for poly(4NPMA) and 4NPMA-co-LIM. The physical properties of homopolymer of NPMA and its copolymer with D-Limonene were compared and evaluated. Thermal stabilities of homo and copolymer were investigated.

Keywords: poly(4NPMA), 4NPMA-co-LIM, density functional theory (DFT), frontier orbital analysis, MEP

DOI: 10.1134/S0036024421010052

1. INTRODUCTION

The synthesis of homopolymers and copolymers with functional active groups as substitutes added to the main chain is an interesting topic [1–5], since copolymerization a successful method for preparation of materials with desired functional properties [6]. Polymers with different properties are obtained especially when functional methacrylamide and methacrylate monomers are employed. Optical clarity is the most distinctive feature of the methacrylate polymers. High light transmittance as well as mechanical and thermal resistance provides them a wide range of applications [7]. Similarly, polymethacrylamide derivatives are known as water-soluble polymers in various applications such as biomedicals, and the methacrylate derivative and *N*-(2-hydroxypropyl) methacrylamide polymer are used in the production of anticancer drugs [8]. Recently, phenyl methacrylate have attracted great attention as potential advanced materials used in many industry applications, such as reagents and electro-active polymers [9, 10], photoionization applications [11], peptide synthesis [12], thermotropic liquid crystal formation [13], methacrylic copolymer adhesives commonly used in wood and leather industries [14, 15], photoresist [16], light sensitive materials [17], biomaterials [18], optical telecommunication materials [19].

Synthetic polymers are mainly obtained from oil and petroleum derivatives. The limited availability of petroleum-based polymer raw materials in the production of polymeric materials creates problems in terms of cost and sustainability. Therefore, interest in natural polymer sources is increasing. Limonene monomer is an important object of study for natural polymer resources [20]. In the literature, there are many studies on the polymerization of limonene [21–27]. In a recent study, it has been found that a newly synthesized limonene-derived biomaterial (poly(limonene)dicarbonate) had the most glass transition temperature ever known. This study shows that limonene could replace potentially carcinogenic Bisphenol-A in the polycarbonates [28]. D-Limonene is a flammable, volatile liquid immiscible with water [29]. Limonene is found in more than 90% of citrus essential oils and is known as the main flavor component of orange. The limonene molecule ($C_{10}H_{16}$) can be found in two forms: D-limonene and L-limonene, which are symmetrical to each other, and have a pleasant odor. L-Limonene smells like pine, and D-limonene smells like orange-lemon [30, 31]. In this study, we synthesized a sustainable polymer from limonene, a natural monomer. For the synthesis of green chemistry, primarily the natural monomer D-limonene and the

N-(4-nitrophenyl) methacrylamide (4NPMA) monomer previously synthesized by our team were used. Thus, we obtained a new green synthesis polymer, which we encoded as 4NPMA-co-LIM.

In the present study we performed homopolymerization of *N*-(4-nitrophenyl)methacrylamide (4NPMA) (poly(4NPMA)) and copolymerization of D-limonene with 4NPMA (4NPMA-co-LIM). The synthesized poly(4NPMA) and 4NPMA-co-LIM were characterized by spectroscopic methods (FT-IR, ^{1}H, and ^{13}C NMR). The vibrational wavenumbers, electronic properties, molecular electronic potential and chemical shifts of these polymers were calculated at DFT/B3LYP/6-311++G(*d*,*p*) level. In addition, Mulliken charge analysis and molecular electrostatic potential (MEP) of molecules were performed. The physical properties of homopolymer of NPMA and its copolymer with D-limonene were compared and evaluated. In addition, the thermal characterization of homo and copolymer was made and its molecular weight was also determined.

2. EXPERIMENTAL

2.1. Materials

The chemicals used for monomer synthesis were purchased from Aldrich, where methacryloyl chloride, *p*-nitroaniline, and trimethylamine were used as is. The chemicals used for homo and copolymer synthesis were purchased from Merck, where *N*,*N*-dimethylformamide and dimethyl sulfoxide were used as a solvent, benzoyl peroxide as a initiator, D-limonene and 4NPMA as monomers.

2.2. Measurements

The FTIR spectra of all samples were performed with a PerkinElmer Spectrum Two (UATR) IR spectrometer in the range of 4000–450 cm^{-1}. ^{1}H and ^{13}C NMR measurements were conducted on AVENCE III Bruker and Bruker Top Spin Ultra Shilt 400 MHz in DMSO-d_6 as solvent. The molecular weight of the polymer was determined by using gel permeation chromatography (GPC) on Agilent 1200 GPC, methyl methacrylate standards. Thermal analsis of the polymer was performed using Hitachi 7000 TGA/DTA/DTG simultaneous system a heating rate of 10°C min^{-1} in nitrogen atmosphere, from room temperature to 550°C.

2.3. Synthesis of Homopolymer poly(4NPMA) and Copolymer NPMA-co-LIM

4NPMA monomer was synthesized and characterized according to the literature [32, 33]. The poly(4NPMA) was polymerized with the benzoyl peroxide initiator in *N*,*N*-dimethylformamide solvent.

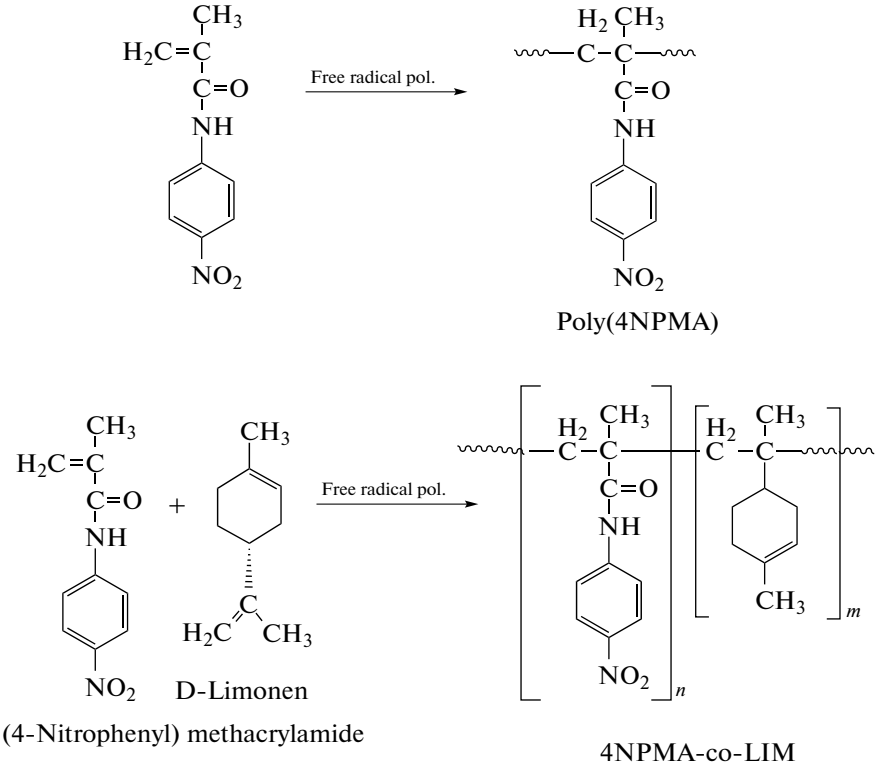

Fig. 1. Synthesis of poly(4NPMA) and 4NPMA-co-LIM.

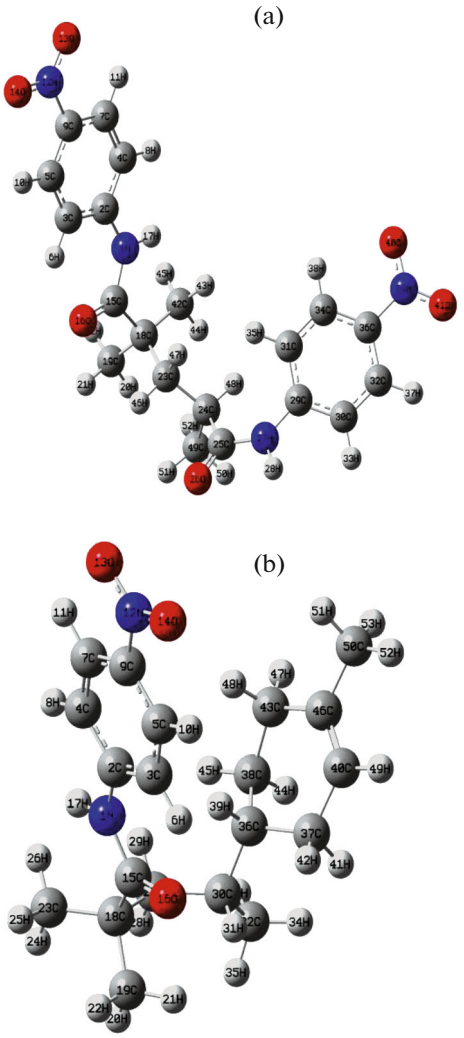

Fig. 2. The optimized structures poly(4NPMA) and 4NPMA-co-LIM.

4NPMA and D-limonene, with the radical initiator benzoyl peroxide in dimethyl sulfoxide solution were added into polymerization flask. The system was kept under inert gas at 70°C in 24 h. The obtained copolymer was precipitated several times to remove impurities with ethyl alcohol. Synthesis of homopolymer poly(4NPMA) and copolymer of limonene with 4NPMA (4NPMA-co-LIM) are shown in Fig. 1, respectively. The chemical structure of homo and copolymer was characterized by spectroscopic methods, FT-IR and NMR.

2.4. Calculation Details

All calculations for the homopolymer and the copolymer were made using the Gaussian package program [34] and the results were visualized with the help of the GaussView 5 [35] program. First, the homopolymer and copolymer molecules were optimized using the DFT/B3LYP method [36] and the 6-311++G(*d*,*p*) basis set [37], then using the optimized results, structural geometric parameters of molecules, vibrational frequencies (FT-IR) and NMR spectra (^{1}H and ^{13}C) were calculated using GIAO approach. These frequencies were multiplied by the scaling factor 0.9982 [38] to approximate the calculated vibrational frequencies to the experimental vibrational frequencies. Many parameters such as HOMO–LUMO energies, chemical hardness, electronegativity and electrophilicity were calculated in the gas phase using the time-dependent TD-B3LYP method. Molecular electrostatic potential surface (MEP) and Mulliken atomic charges of homopolymer and copolymer were investigated.

3. RESULTS

3.1. Structural Analysis

In order to understand the structure of the homo and copolymer, the molecules were optimized by the DFT/B3LYP/6-311++G(*d*,*p*) method. Optimized geometrical structures are shown in Fig. 2. The bond lengths, bond angles and dihedral angles of similar sides of these structures are given in Table 1, which also shows the crystal data of the 4-nitrophenyl methacrylate molecule for comparison [39], which has a similar structure to the 4NPMA monomer. It is seen that there is agreement between similar structures except for some differences (R-square, 0.9992 for poly(4NPMA) and 0.9025 for 4NPMA-co-LIM, respectively).

3.2. Vibrational Spectrum

The basic vibrational frequencies of the poly(4NPMA) and 4NPMA-co-LIM molecules were calculated using the B3LYP method and the 6-311++G(*d*,*p*) basis set. The experimental IR spectrum was measured with a PerkinElmer Spectrum Two FT-IR spectrometer in the wavenumber range of 4000–450 cm^{-1}. Experimental Fourier Transform Infrared (FT-IR) frequencies and theoretical infrared spectra are given in Figs. 3 and 4.

The spectral bands of these vibrational spectra are listed in Table 2 for poly(4NPMA), and Table 3 for 4NPMA-co-LIM. The most characteristic peaks observed in FT-IR spectrum of poly(4NPMA) and 4NPMA-co-LIM are: for poly(4NPMA) and 4NPMA-co-LIM homo and copolymers, the C=C-stretch band on the aromatic ring was observed at 1614 and 1616 cm^{-1}, respectively. For poly(4NPMA) molecule, C=O amide stretch appears at 1685 cm^{-1}, for 4NPMA-co-LIM this band was observed at 1673 cm^{-1} [40, 41]. N–H bending vibrational was shown at 1594 cm^{-1} for poly(4NPMA), this bending vibrational was observed at 1595 cm^{-1} for 4NPMA-co-LIM. The

Table 1. Some selected optimized geometric parameters of the poly(4NPMA) and 4NPMA-co-LIM (Å, deg)

Bond lengths	Poly (4NPMA)	4NPMA-co-LIM	4-Nitrophenyl methacrylate [40]	Bond angles	Poly (4NPMA)	4NPMA-co-LIM	4-Nitrophenyl methacrylate [40]
N1–C2	1.422	1.470		C2–N1–C15	126.088	120.000	—
N1–C15	1.420	1.470	—	C2–N1–H17	115.524	120.000	—
N1–H17	1.026	1.000	—	C15–N1–H17	118.385	120.000	—
C2–C3	1.411	1.395	1.384	N1–C2–C3	122.690	119.997	—
C2–C4	1.418	1.395	1.381	N1–C2–C4	117.141	120.004	—
C3–C5	1.389	1.395	1.381	C3–C2–C4	120.169	119.999	122.41
C3–H6	1.098	1.100	0.95	C2–C3–C5	119.759	120.009	118.58
C4–C7	1.388	1.395	1.385	C2–C3–H6	120.293	119.981	120.70
C4–H8	1.089	1.100	0.95	C5–C3–H6	119.944	120.011	120.70
C5–C9	1.407	1.395	1.385	C2–C4–C7	119.826	120.000	119.11
C5–H10	1.097	1.100	0.95	C2–C4–H8	120.838	120.008	120.40
C7–C9	1.407	1.395	1.382	C7–C4–H8	119.336	119.992	120.40
C7–H11	1.098	1.100	0.95	C3–C5–C9	119.876	119.994	119.00
C9–N12	1.470	1.470	1.466	C3–C5–H10	120.663	120.013	120.50
N12–O13	1.221	1.199	1.231	C9–C5–H10	119.461	119.993	120.50
N12–O14	1.222	1.199	1.224	C4–C7–C9	119.654	120.005	118.42
C15–O16	1.214	1.258	—	C4–C7–H11	120.827	119.984	120.80
C15–C18	1.553	1.540	—	C9–C7–H11	119.520	120.011	120.80
C18–C19	1.538	1.540	—	C5–C9–C7	120.715	119.994	122.47
C18–C23	1.540	1.540	—	C5–C9–N12	119.614	119.981	118.62
C18–C42	1.540	1.540	—	C7–C9–N12	119.670	120.025	118.91
C19–H20	1.070	1.070	—	C9–N12–O13	117.733	118.393	118.22
C19–H21	1.070	1.070	—	C9–N12–O14	117.608	118.393	118.44
C19–H22	1.070	1.070	—	O13–N12–O14	124.659	123.214	123.34
C23–C24	1.540	1.070	—	N1–C15–O16	121.006	120.227	—
				N1–C15–C18	116.714	119.887	—
				O16–C15–C18	122.240	119.887	—

Table 2. Comparisons of experimental and theoretical FT-IR, ^{1}H, and ^{13}C-NMR spectra of poly(4NPMA)

FT-IR (exp.)		DFT	^{1}H-NMR (exp.)		^{13}C-NMR (exp.)	
vibration types	wavenumbers (cm^{-1})		type	δ(ppm)	type	δ (ppm)
					O=C–NH	173
C=C aromatic ring stretch	1614	1582 and 1587	Ring protons	7.5 and 7.9	Ring carbons	119, 124, 142, 145
C=O amide stretch	1685	1687 and 1693			C–CH_3	29
N–H bending	1594	1495, 1523, 1530, 1591, 1687, 1693	N–H	10.2		
NO_2 stretch	1500 (asymmetric) 1330 (symmetric)	1523 (asymmetric) 1320 (symmetric)	Polymer chain –H	1.5	Polymer chain –C	35 and 42

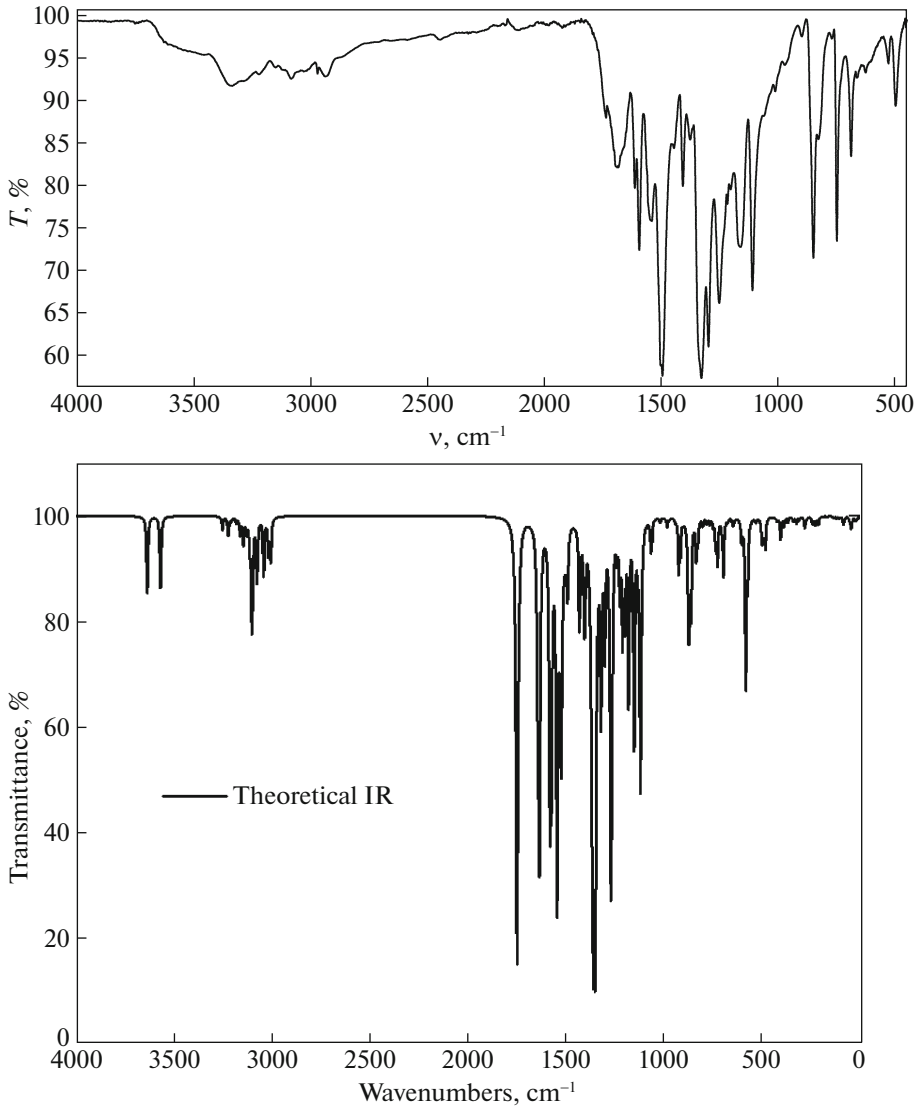

Fig. 3. The experimental and theoretical FTIR spectra of poly(4NPMA).

N–H stretching vibrational of 4NPMA-co-LIM observed at 3279 cm^{-1}. Similarly antisymmetric and symmetric stretch NO_2 were measured at 1500 and 1330 cm^{-1} for poly(4NPMA) and 1496 and 1332 cm^{-1} for 4NPMA-co-LIM. In spectroscopic methods such as FT-IR and NMR, the peaks of molecules with the same functional group give peaks in close proximity to each other. All functional groups linked to the molecule are affected by each other. Slightly shifting of the peak areas of molecules with similar functional group is expected. Calculated vibrational frequencies for both molecules are presented in Tables 2 and 3 and compared with their experimental data. Although there are some differences between the results, they are generally in agreement (R-square, 0.9992 for poly(4NPMA) and 0.9025 for 4NPMA-co-LIM, respectively). While the experimental measurements were performed with the solid material, the theoretical calculations were made for the gas phase.

3.3. Nuclear Magnetic Resonance Analysis

Experimental nuclear magnetic resonance (NMR) spectra were obtained on a Bruker 400 MHz spectrometer in dimethyl sulfoxide-d_6 (DMSO-d_6). The theoretical chemical shiftvalues were calculated in dimethyl sulfoxide (DMSO) by using the Gauge independent atomic orbital (GIAO) method at B3LYP/6-311++G(*d*,*p*) level of theory. Theoretically calculated ^{13}C NMR shifts were compared to experimental data before they were scaled with the equation

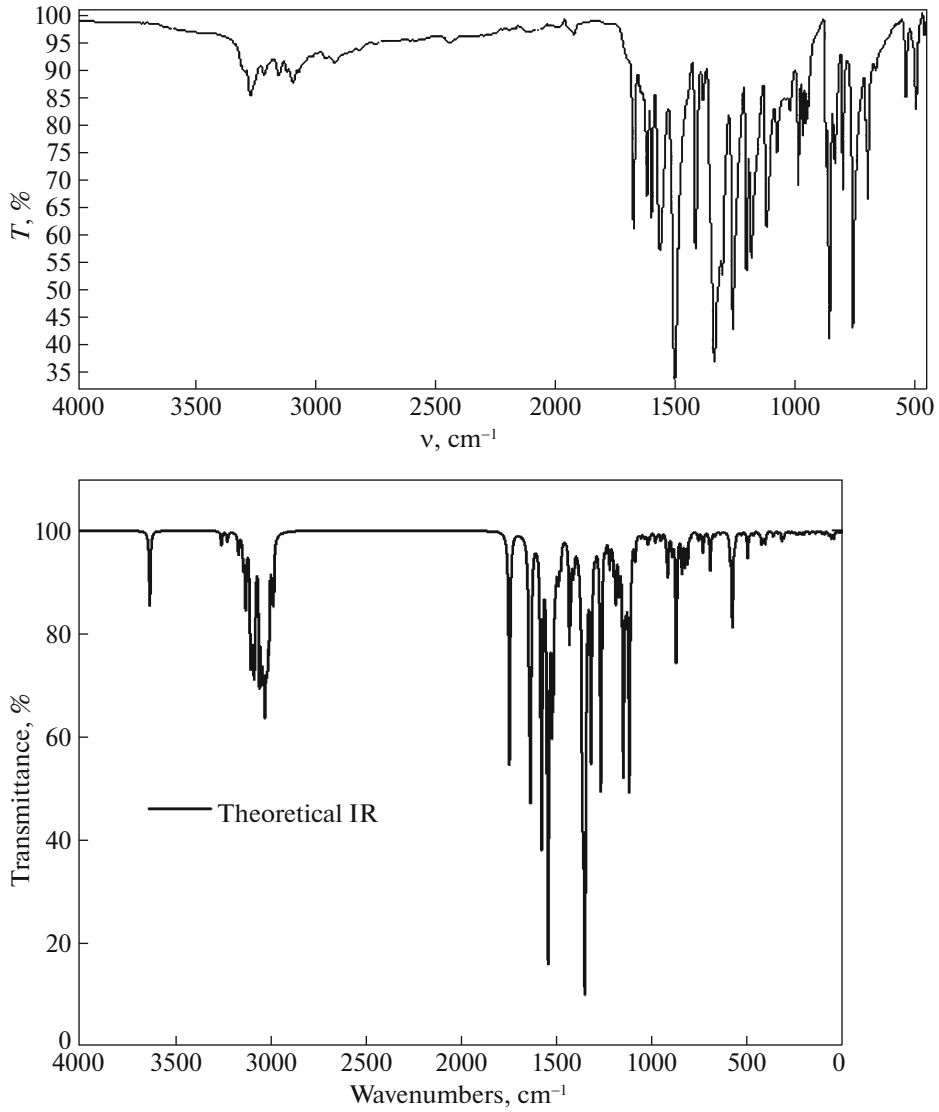

Fig. 4. The experimental and theoretical FTIR spectra of 4NPMA-co-LIM.

$\delta_{scal} = 0.95\delta_{calc} + 0.30$ [42]. ^{1}H and ^{13}C NMR spectra for poly(4NPMA) and 4NPMA-co-LIM in Figs. 5 and 6; and NMR chemical shift values are given in Tables 4 and 5.

Experimental shifts prepared in DMSO-d_6 solvent and shown in Table 4 are observed and calculated as following peaks: ^{1}H-NMR spectrum for poly(4NPMA); N–H structure at 10.2 ppm, aromatic ring protons at 7.9 and 7.5 ppm, polymer chain protons at 1.5 ppm. Theoretical ^{1}H chemical shifts are calculated in the ranges 8.73–1.03 ppm. Theoretical and experimental results comply with each other in general (R-square, 0.8188). Some atoms were affected by electronegative atoms such as oxygen and nitrogen in their vicinity and showed a higher chemical shift. ^{13}C-NMR spectrum for poly(4NPMA), the following peaks; at 173 ppm for O=C–NH, at 29 ppm for C–CH_3, ring carbons at 119, 124, 142, and 145 ppm, polymer chain carbons at 35 and 42 ppm. Theoretical ^{13}C chemical shifts are calculated in the ranges 176–21 ppm. Experimental and theoretical results are compatible with each other (R-square, 0.9914). In the literature, aromatic carbons give resonance between 100 and 150 ppm and give signals in overlapping regions of the spectrum, but by adding electron donating and electron withdrawing substituents, all resonance aromatic carbon expands to 90–180 ppm carbon [43, 44].

The experimental and theoretical ^{1}H-NMR spectrum for 4NPMA-co-LIM given in Table 5 are as follows: N–H-structure at 10.8 ppm, ring protons at 8.2–7.9 ppm, endocyclic and exocyclic –CH cyclohexene protons at 6.5 and 5.8 ppm, CH_2 cyclohexene

Table 3. Comparisons of experimental and theoretical FT-IR and ^{1}H-NMR spectra of 4NPMA-co-LIM

FT-IR (exp.)		DFT	^{1}H-NMR (exp.)	
vibration types	wavenumbers (cm^{-1})		type	δ (ppm)
C=C aromatic ring stretch	1616	1610 and 1615	Ring protons	7.9 and 8.2
C=O amide stretch	1673	1656	Endocyclic and exocyclic	6.5 and 5.8
N–H stretch	3279	3250	N–H	10.8
N–H bending	1595	1495, 1500	Polymer chain $-CH_2$ and $-CH_3$	2.4–2.6 and 1.2
NO_2 stretch	1496 (asymmetric) 1332 (symmetric)	1322 and 1224	Cyclohexene CH_2	2.5–2.7
			Limonene CH_3	2.0

Table 4. The chemical shift in ^{1}H and ^{13}C NMR spectra of poly(4NPMA)

Atoms	Experimental (ppm)	Theoretical (ppm)	Atoms	Experimental (ppm)	Theoretical (ppm)	Atoms	Experimental (ppm)	Theoretical (ppm)
C25	173	176	C18	42	48	H28	10.2	7.03
C15	173	174	C23	35	46	H8	7.5	6.75
C29	145	145	C24	42	36	H48	1.5	2.77
C2	145	144	C19	29	29	H47	1.5	2.75
C36	140	143	C42	29	22	H51	1.5	1.41
C9	140	143	C49	29	21	H43	1.5	1.34
C5	124	124	H6	7.9	8.73	H50	1.5	1.32
C34	124	124	H37	7.5	8.40	H52	1.5	1.29
C7	124	124	H11	7.9	8.32	H20	1.5	1.24
C32	124	124	H10	7.5	8.27	H22	1.5	1.16
C31	119	120	H38	7.9	8.14	H45	1.5	1.15
C30	119	119	H17	10.2	7.47	H46	1.5	1.08
C4	119	116	H33	7.9	7.34	H44	1.5	1.05
C3	119	115	H35	7.5	7.07	H21	1.5	1.03

at 2.5–2.7 ppm, polymer chain $-CH_2$ at 2.4–2.6 ppm, polymer chain $-CH_3$ at 1.2 ppm, and limonene CH_3 at 2.0 ppm. Theoretical ^{1}H chemical shifts are calculated in the ranges 7.9–1.2 ppm.

3.4. Frontier Molecular Orbitals (FMOs)

Figure 7 shows the shape of the molecular orbital (MOs) of poly(4NPMA) and 4NPMA-co-LIM molecules called HOMO and LUMO at TD-DFT/B3LYP/6-311++G(*d*,*p*) level. The boundary molecular orbital (FMO) of a molecule, HOMO (highest full molecular orbital) and LUMO (lowest empty molecular orbital), is important in terms of properties such as electronic, optical, chemical reactivity, molecular stability of the molecule [45–47]. HOMO energy is related with electron donation potential, while LUMO energy is related with electron receiving [48]. In other words, electrons can be easily separated from the HOMO orbital in terms of

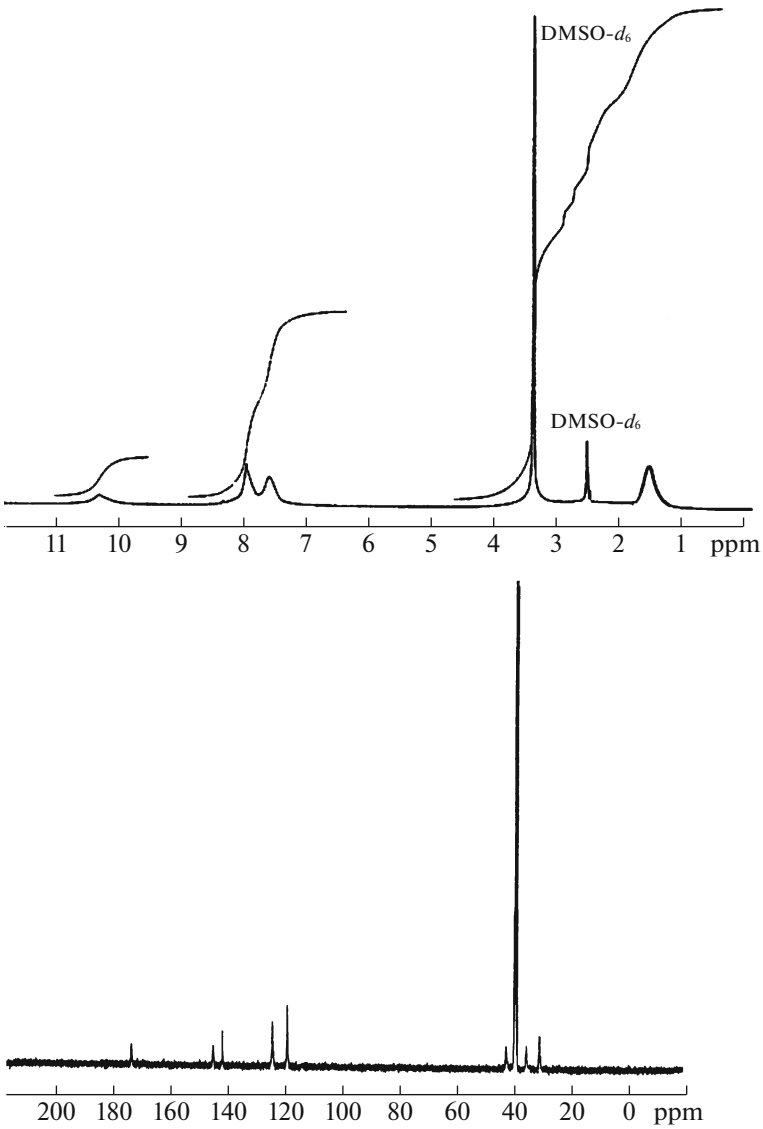

Fig. 5. ^{1}H and ^{13}C spectra of poly(4NPMA).

energy, while they can easily settle into the LUMO orbital. The difference between HOMO–LUMO energy values is also important for the electrical conductivity and intermolecular charge distribution of the molecule.

Moreover, MO theory often used by chemists is important in describing terms such as chemical potential (μ), ionization potential (I), electronegativity (χ), electron affinity (A), electrophilicity index (w), hardness (η), and softness (S). Koopmans [49] defines closed shell components η, μ, and χ as $\eta = I - A$, $\mu = (I - A)/2$, $\chi = (I + A)/2$. Electron affinity and ionization potential can be estimated through HOMO and LUMO orbital energies as $A = -E_{LUMO}$ and $I = -E_{HOMO}$. The electronegativity and chemical hardness are often used to make chemical reactivity prediction. Also, a molecule with small frontier orbital gap is named as a soft molecule. Soft molecules are more polarizable and have a high chemical reactivity as well as low kinetic stability [50]. The poly(4NPMA) molecule is $E_{HOMO} = -7.54$ eV, the $E_{LUMO} = -3.22$ eV, the 4NPMA-co-LIM molecule is $E_{HOMO} = -6.46$ eV, $E_{LUMO} = -2.73$ eV. Other parameters such as ionization potential, electron affinity, electronegativity, chemical potential, chemical hardness and softness and electrophilicity index of poly(4NPMA) and 4NPMA-co-LIM molecules are presented in Table 6. The energy gap value of poly(4NPMA) is $E_{gap} = 4.02$ eV, the energy gap of 4NPMA-co-LIM is $E_{gap} = 3.73$ eV. In a previous study, the energy gap of 4NPMA monomer was calculated as 4.30 eV. After the homopolymer process of NPMA, this value decreased

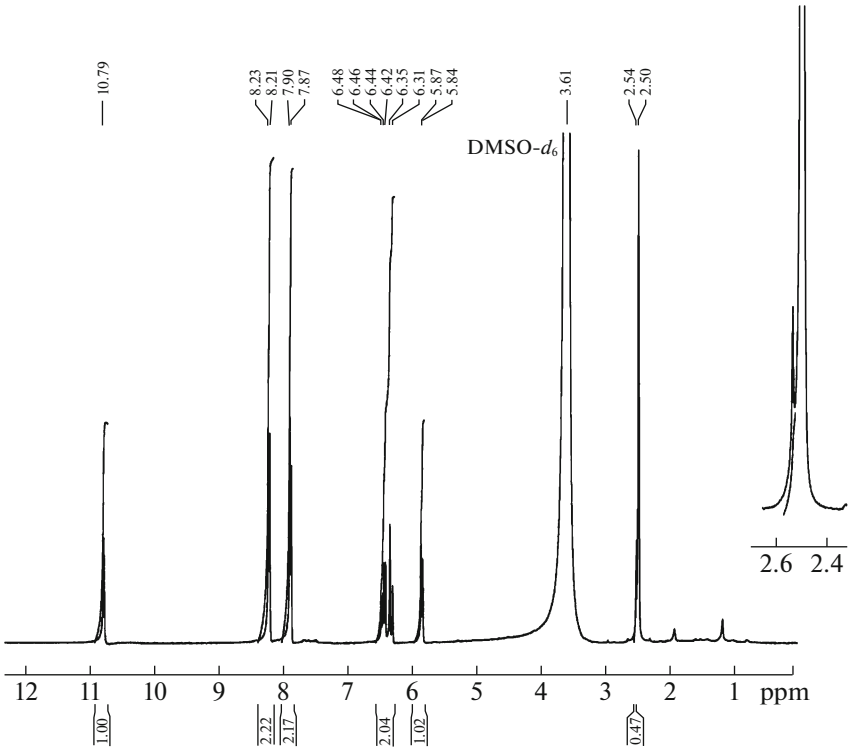

Fig. 6. ^{1}H-NMR spectrum of 4NPMA-co-LIM.

to 4.02 eV, after the copolymer process of NPMA with D-limonene decreased to 3.73 eV. Therefore, it can be said that the conductivity of the copolymer is better than the homopolymer. It can also be said that both molecules have a semiconductor energy band gap. The chemical potential values of poly(4NPMA) and

Table 5. The chemical shift in ^{1}H and ^{13}C NMR spectra of 4NPMA-co-LIM

Atoms	Experimental (ppm)	Theoretical (ppm)	Atoms	Experimental (ppm)	Theoretical (ppm)	Atoms	Experimental (ppm)	Theoretical (ppm)
C15		175.30	C38		23.87	H31	1.5	1.60
C2		145.35	C50		23.16	H45	2.5–2.7	1.55
C9		143.67	C19		22.77	H53	2.0	1.51
C46		137.28	C32		16.20	H52	2.0	1.46
C5		124.82	H6	7.9	9.05	H51	2.0	1.35
C7		124.45	H11	8.2	8.38	H25	2.4–2.6	1.30
C40		121.66	H10	8.2	8.32	H26	2.4–2.6	1.24
C4		116.08	H17	10.8	7.81	H28	2.4–2.6	1.14
C3		114.57	H8	7.9	7.00	H44	2.5–2.7	1.13
C27		47.71	H49	5.8	5.56	H24	2.4–2.6	1.13
C18		47.21	H21	1.2	1.95	H22	1.2	1.02
C36		39.68	H41	2.5–2.7	1.92	H39	0.5	0.93
C30		34.41	H29	2.4–2.6	1.81	H34	2.0	0.87
C43		32.87	H47	2.5–2.7	1.70	H35	2.0	0.71
C37		32.69	H48	2.5–2.7	1.64	H33	2.0	0.65
C23		26.51	H42	2.5–2.7	1.63	H20	1.2	0.56

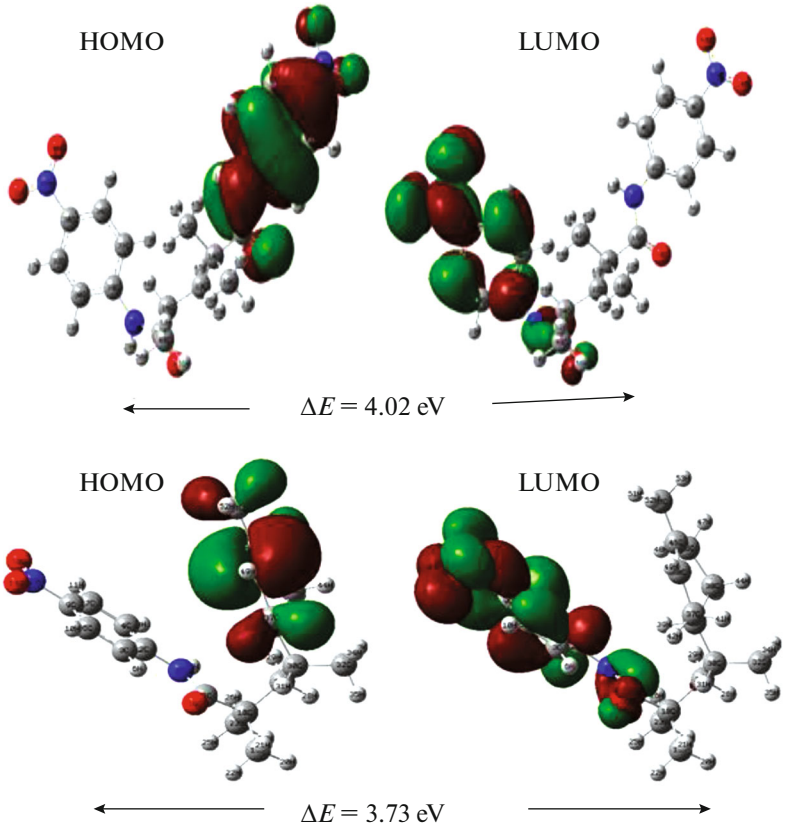

Fig. 7. Frontier molecular orbitals of poly(4NPMA)and 4NPMA-co-LIM, respectively.

4NPMA-co-LIM are −5.23 and −4.60 eV, respectively. It is more stable than poly(4NPMA) 4NPMA-co-LIM in terms of both energy gap value and chemical potential. Furthermore, since the 4NPMA-co-LIM molecule's energy range is smaller than that of poly(4NPMA), 4NPMA-co-LIM is softer and better polarized.

Table 6. The calculated energies values of the poly(4NPMA) and 4NPMA-co-LIM

Energies values	Poly(4NPMA)	4NPMA-co-LIM
E_{HOMO} (eV)	−7.24	−6.46
E_{LUMO} (eV)	−3.22	−2.73
Ionization potential (eV)	7.24	6.46
Electron affinity (eV)	3.22	2.73
Energy gap (eV)	4.02	3.73
Electronegativity (eV)	5.23	4.60
Chemical potential (eV)	−5.23	−4.60
Chemical hardness (eV)	2.01	1.86
Chemical softness (eV^{-1})	0.25	0.27
Electrophilicity index (eV)	6.80	5.66

3.5. Molecular Electrostatic Potential (MEP) Analysis

The MEP surface diagrams of the molecules are useful in the investigation of molecular structure with positive, negative and neutral electrostatic potential regions due to color grading [51, 52]. It is a frequently used calculation technique to decide effects such as nucleophilic and electrophilic attacks in a molecule. In this visual presentation of chemical activity, the negative (red) regions of the MEP relate to the electrophilic reactivity (electron-donating reaction) and the positive (blue) regions of the nucleophilic reactivity (electron receiving reaction). MEP studies for both molecules were performed using the basic set of B3LYP/6-311++G(*d*,*p*) and shown in Fig. 8. All colors in this range from red to blue were used. Following is the color legend on the MEP surface: red color shows electronically rich region, while partly negative charge is shown as blue color for electron-deficient region, partly positive charge is depicted as light blue color for lightly electron deficient region, yellow color marks lightly

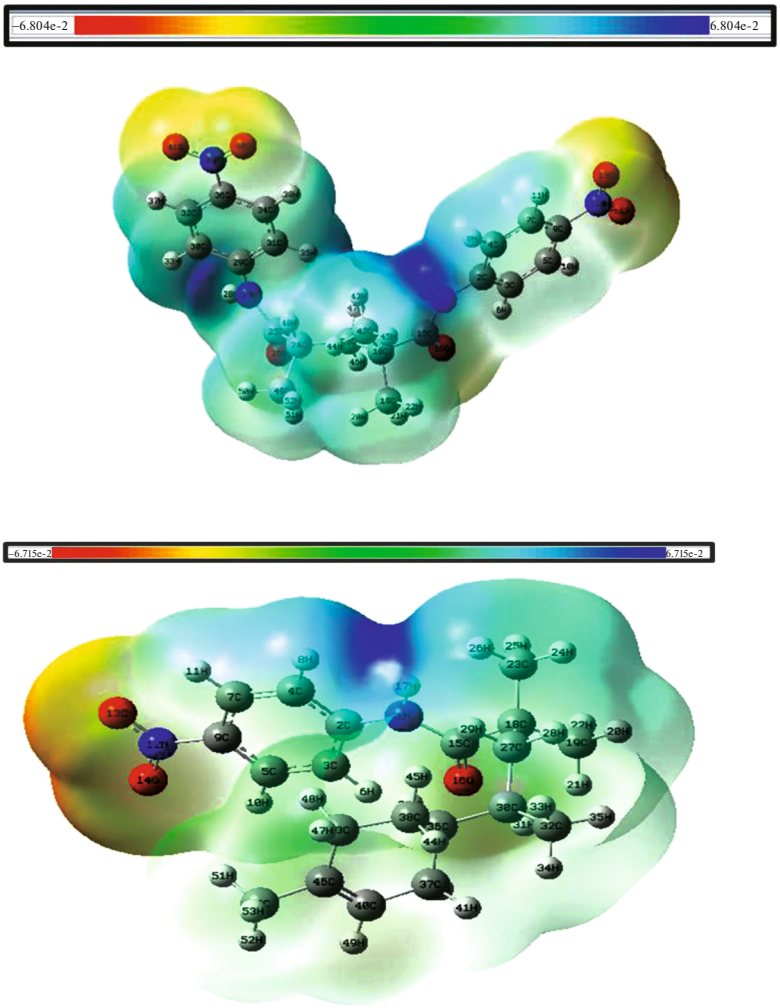

Fig. 8. MEP surface diagrams of the molecules of poly(4NPMA) and 4NPMA-co-LIM, respectively.

electron rich region, and green color means neutral. In this study, color coding is between −0.06804 (dark red) and 0.06804 (dark blue) for poly(4NPMA), −0.06715 and 0.06715 for 4NPMA-co-LIM. As seen from the MEPs, while the region near the CH groups have positive potential, the regions over the oxygen atoms have negative potential for poly(4NPMA) and 4NPMA-co-LIM.

3.6. Mulliken Atomic Charge

Mulliken atomic charges obtained from Mulliken population analysis are given in Fig. 9 and Tables 7 and 8 for poly(4NPMA) and 4NPMA-co-LIM. The atomic charge distribution gives information about the donor-acceptor atoms and the electronic charge distribution of the molecule. H29 and H39 atoms for poly(4NPMA) and 4NPMA-co-LIM molecules are positive for all H atoms except H9 and H39 atoms. The highest positive charge for poly(4NPMA) belongs to H17 atom and C36 for 4NPMA-co-LIM. The lowest negative charge for poly(4NPMA) belongs to the atom O41, for the 4NPMA-co-LIM to the C5 atom.

3.7. Thermal and Chromatographic Characterization of Homo and Copolymer

Molecular weight and molecular weight distribution of homo and copolymer were detected by GPC (Gel Permeation Chromatography). The highest molecular weight of the poly(4NPMA) (weight-average molecular weight $\overline{M_w}$ = 16146, number-average molecular weight $\overline{M_n}$ = 15510 g/mol) was determined and polydispersity index (PDI) of homopolymer $\overline{M_w}/\overline{M_n}$ = 1.041; the highest molecular weight of the 4NPMA-co-LIM (weight-average molecular weight $\overline{M_w}$ = 16456, number-average molecular weight

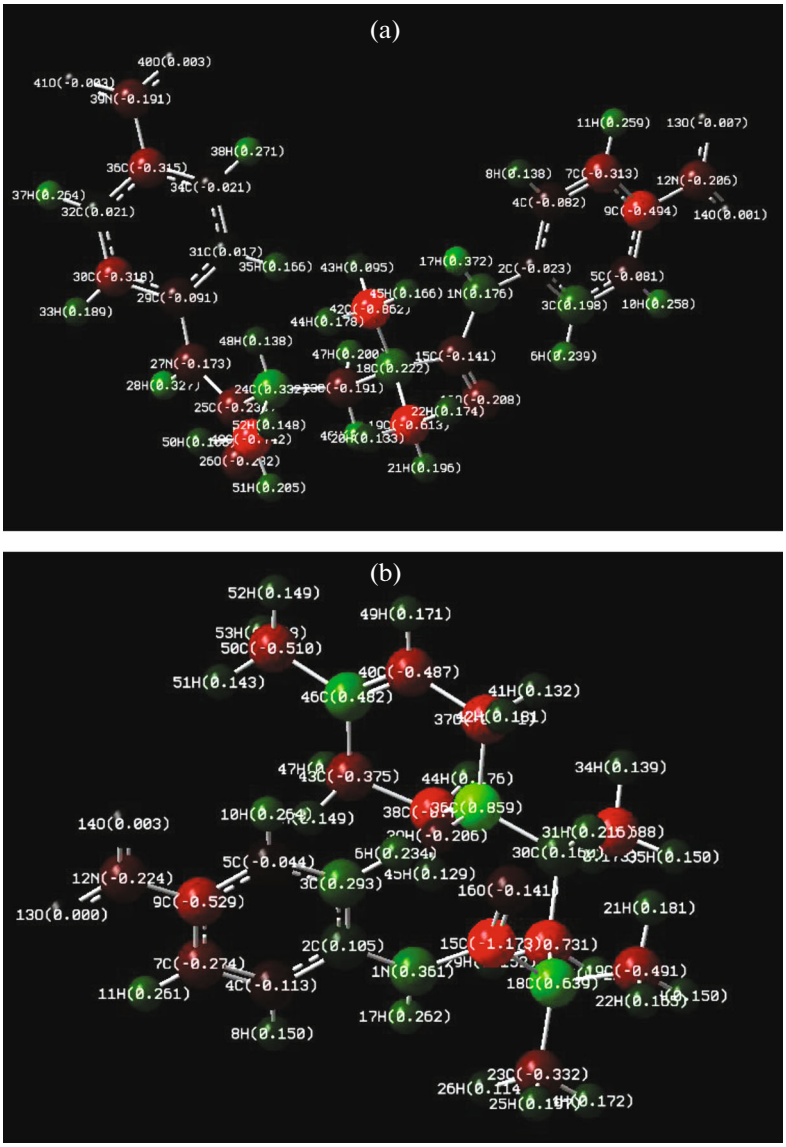

Fig. 9. Mulliken atomic charges of poly(4NPMA) and 4NPMA-co-LIM, respectively.

$\overline{M_n}$ = 15736 g/mol) was determined and PDI of copolymer $\overline{M_w}/\overline{M_n}$ = 1.046 detected by GPC.

Thermal analysis methods help determining the thermal stabilities of polymer and provide information about their thermal behavior. The thermal properties of polymer are determined by TGA/DTA/DTG (thermal gravimetric analysis/differential thermal analysis/differential thermogravimetric analysis) simultaneous system. The decomposition temperature and the temperature at weight loss are taken as a measure of thermal stability. The degradation of the homopolymer from the thermogram was observed at two levels and the copolymer was observed at three levels. The thermal curves of the polymers are given in Fig. 10 and Table 9 [53].

4. DISCUSSION

In this study, a new sustainable-green polymer synthesis from limonene, a natural monomer, was realized. 4NPMA-co-LIM as green polymer and poly(4NPMA) were synthesized and characterized by FT-IR, ^{1}H, and ^{13}C-NMR spectroscopy techniques. Both experimental and theoretical methods showed that the polymers were successfully synthesized. The results showed that the calculated frequencies corresponded to the experimental values except for some deviations. While the experimental measurements of these differences were taken as solid, the theoretical calculations were made in the gas phase. These deviations are also thought to be due to the harmonic approach used. Furthermore, these differences result

Table 7. Mulliken atomic charges of the poly(4NPMA)

Atoms	Charges	Atoms	Charges
N1	0.176	H28	0.327
C2	–0.023	H29	–0.091
C3	0.198	C30	–0.318
C4	–0.082	C31	0.017
C5	–0.081	C32	0.021
H6	0.239	H33	0.189
C7	–0.313	C34	–0.021
H8	0.138	H35	0.166
C9	–0.494	C36	–0.315
H11	0.259	H37	0.264
N12	–0.206	H38	0.271
O13	–0.007	N39	–0.191
O14	0.001	O40	0.003
C15	–1.141	O41	–0.003
O16	–0.208	C42	–0.862
H17	0.372	H43	0.095
C18	0.222	H44	0.178
C19	–0.613	H45	0.166
H20	0.133	H46	0.302
H21	0.196	H47	0.200
H22	0.174	H48	0.138
C23	–0.191	C49	–0.742
C24	0.332	H50	0.156
C25	–0.236	H51	0.205
O26	–0.232	H52	0.148
N27	–0.173		

Table 8. Mulliken atomic charges of the 4NPMA-co-LIM

Atoms	Charges	Atoms	Charges
C7	–0.274	H28	0.210
H8	0.150	H29	0.152
H9	–0.529	C30	0.160
H10	0.264	H31	0.216
H11	0.261	C32	–0.688
N12	–0.224	H33	0.173
O13	0.000	H34	0.139
O14	0.003	H35	0.150
C15	–1.173	C36	0.859
O16	–0.141	C37	–0.621
H17	0.262	C38	–0.732
C18	0.639	H39	–0.206
C19	–0.491	C40	–0.487
H20	0.150	H41	0.132
H21	0.181	H42	0.181
H22	0.165	C43	–0.375
C23	–0.332	H44	0.176
H24	0.172	H45	0.129
H25	0.197	C46	0.482
H26	0.114	H47	0.200
C27	–0.731	H48	0.149

Table 9. Thermal data of the poly(4NPMA) and 4NPMA-co-LIM

Sample	Max. decomposition temperature (°C)	Temp. of 10% weight loss (°C)	Temp. of 25% weight loss (°C)	Temp. of 50% weight loss (°C)	Weight loss, % (400°C)	Weight loss, % (500°C)	Residue, % (550°C)
Poly(4NPMA)	302	285	310	461	44	53	44
4NPMA-co-LIM	247	242	301	447	45	55	42

from the intramolecular and non-molecular interaction of poly(4NPMA) and 4NPMA-co-LIM hydrogen bonds. HOMO–LUMO energies and also other related molecular properties have been calculated to have more information about the molecule. The energy gap value of poly(4NPMA) is $E_{gap} = 4.02$ eV, the energy gap of 4NPMA-co-LIM is $E_{gap} = 3.73$ eV. After homopolymerization of NPMA, energy gap value decreased to 4.02 eV, after the copolymer process of NPMA with D-limonene decreased to 3.01 eV. Therefore, it can be said that the conductivity of the copolymer is better than that of homopolymer. Also, thermal stability of homo and copolymer was investigated and its molecular weight was determined. We hope that the results of the study could shed light on the development of new materials with both experimental and theoretical evidence in applied sciences.

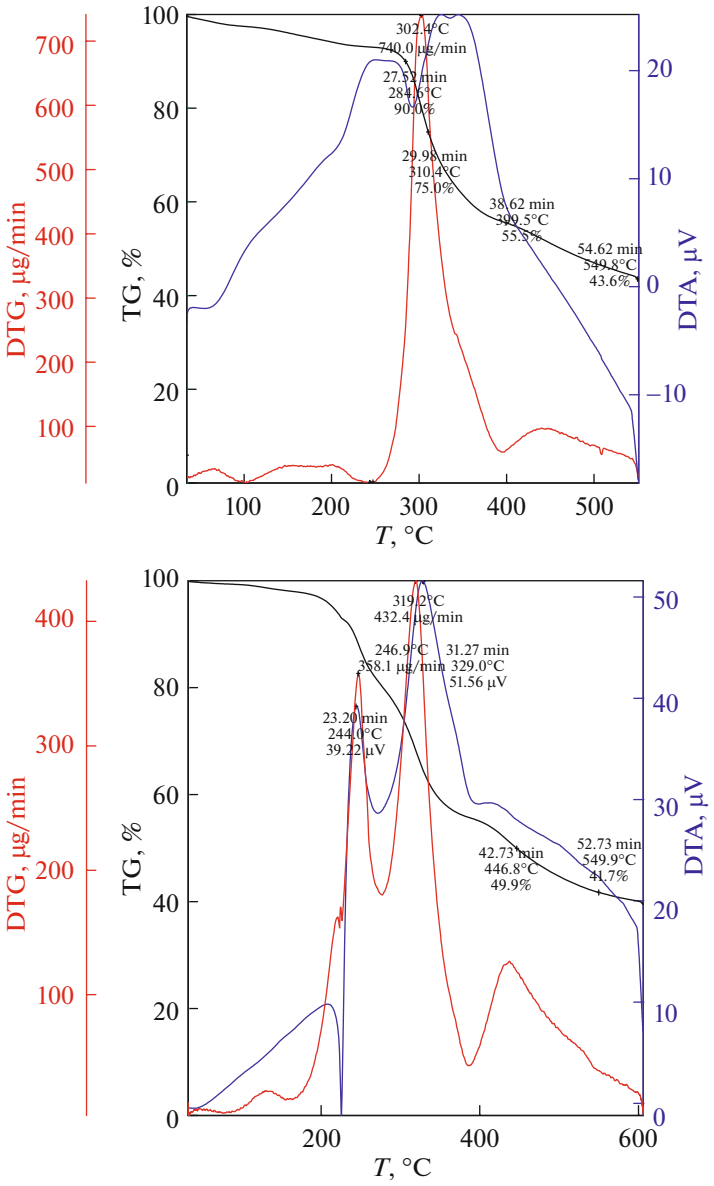

Fig. 10. Thermal curves of poly(4NPMA) and 4NPMA-co-LIM.

ACKNOWLEDGMENTS

The authors thank the University of Usak-Institute of Science. This article is derived from Pembe Gül SAPAN's thesis entitled "Synthesis, Characterization and Molecular Modeling of New Methacrylamide-Containing Monomer and Polymers."

REFERENCES

1. F. Akman, J. Thermoplast. Compos. Mater., 1 (2017).
2. F. Akman, Polymer Bull. **74**, 2975 (2017).
3. F. Akman, NRC Res. Press **94**, 1 (2016).
4. M. Talu, E. U. Demiroğlu, S. Yurdakul, and S. Badoğlu, Spectrochim. Acta, Part A **134**, 267 (2015).
5. F. Akman and N. Çankaya, Pigment Resin Technol. **45**, 301 (2016).
6. M. D. B. Desai, B. S. R. Reddy, R. Arshady, and M. H. George, Polymer **27**, 96 (1986).
7. N. Çankaya and G. Besci, J. Faculty Eng. Archit. Gazi Univ. **33**, 1155 (2018).
8. Y. Wang, F. Ye, E. K. Jeong, Y. Sun, D. P. Parker, and Z. R. Lu, Pharm. Res. **24**, 1208 (2007).
9. P. S. Vijayan and A. Penlidis, J. Mac. Sci-Pure Appl. Chem. **39**, 591 (2002).
10. R. Arshady, B. S. R. Reddy, and M. H. George, Polymer **27**, 769 (1986).
11. S. Pitchumani and C. Rami Reddy, J. Polym. Sci. Polym. Chem. Ed. **20**, 277 (1982).

12. M. Bankova, T. Petrova, N. Manolova, and I. Rashkov, Eur. Polym. J. **32**, 569 (1998).
13. M. Babazadeh, Polym. Deg. Stab. **91**, 3245 (2006).
14. P. S. Vijayanand, R. Arunprasath, R. Balaji, and S. Nanjundan, J. Appl. Polym. Sci. **85**, 2261 (2002).
15. P. G. Vijayaraghavan and B. S. R. Reddy, J. Appl. Polym. Sci. **61**, 936 (1996).
16. K. Ichimura and Y. Nishio, J. Polym. Sci., Part A **25**, 1579 (1987).
17. J. L. Hua and J. W. YipLam, Polymer **47**, 18 (2006).
18. P. G. Vijayaraghavan and B. S. R. Reddy, J. Appl. Polym. Sci. **61**, 936 (1996).
19. C. S. Joneselvamalar and P. S. Vijayanand, J. Appl. Polym. Sci. **91**, 3604 (2004).
20. A. Mohammad, *Properties and Application in Chemistry, Green Solvents I* (Springer, New York, 2012).
21. M. Modena, R. B. Bates, and C. S. Marvel, J. Polym. Sci. A **3**, 949 (1965).
22. W. J. Roberts and A. R. Day, J. Am. Chem. Soc. **72**, 1226 (1950).
23. T. Douichi, H. Yamanguchi, and Y. Minoura, Eur. Polym. J. **17**, 961 (1981).
24. S. Sharma and A. Srivastava, Eur. Polym. J. **9**, 2235 (2004).
25. S. Sharma and A. Srivastava, Polym. Plast. Technol. Eng. **3**, 485 (2003).
26. S. Sharma and A. Srivastava, J. Appl. Polym. Sci. **6**, 593 (2003).
27. Y. Zhang and A. M. Dube, Polym.-Plast. Technol. Eng. **54**, 499 (2015).
28. N. Kindermann, A. Cristofol, and A. W. Kleij, ACS Catal. **7**, 3860 (2017).
29. S. Raeissi and C. J. Peters, J. Supercrit. Fluids **33**, 201 (2005).
30. A. Potter, J. Andersson, A. Sjöblom, E. Junedahl, A. P. Cousins, and E. Lunden, Results from the Swedish National Screening Programme (2004).
31. N. Çankaya, E. Tanış, H. E. Gülbaş, and N. Bulut, Polym. Bull. **76**, 3297 (2019).
32. N. Çankaya and E. Tanış, Mater. Res. Express **6**, 025310 (2019).
33. T. Jähnert, T. Janoschka, M. D. Hager, and U. S. Schubert, Eur. Polym. J. **61**, 105 (2014).
34. M. J. Frisch et al., *Gaussian 09, Revision A.2* (Gaussian, Inc., Wallingford, CT, 2009).
35. R. Dennington, T. Keith, and J. Millam, *GaussView, Version 5* (Semichem Inc.).
36. A. D. Becke, Phys. Rev. A **38**, 3098 (1988).
37. S. H. Vosko, L. Vilk, and M. Nusair, Can. J. Phys. **58**, 1200 (1980).
38. H. Watanabe, N. Hayazawa, Y. Inouye, and S. Kawata, J. Phys. Chem. B **109**, 5012 (2005).
39. Y.-H. Xu and Q. Fanqi, Acta Crystallogr., E **64**, o1751 (2008).
40. M. Barthes, G. D. Nunzio, and M. Ribet, Synth. Met. **76**, 337 (1996).
41. N. P. G. Roeges, *A Guide to the Complete Interpretation of Infrared Spectra of Organic Compounds* (Wiley, New York, 1994).
42. A. E. Aliev, D. Courtier-Murias, and S. Zhou, J. Mol. Struct.: THEOCHEM **893**, 1 (2009).
43. H. O. Kalinowski, S. Berger, and S. Braun, *Carbon-13 NMR Spectroscopy* (Wiley, Chichester, 1988).
44. K. Pihlaja and E. Kleinpeter, *Carbon-13 Chemical Shifts in Structural and Sterochemical Analysis* (VCH, New York, 1994).
45. K. Matyjaszewski, ACS Symp. Ser. **944**, 252 (2006).
46. A. D. Jenkins, R. G. Jones, and G. Moad, Pure Appl. Chem. **82**, 483 (2010).
47. I. Fleming, *Frontier Orbital and Organic Chemical Reactions* (Wiley, New York, 1976).
48. C. S. Abraham, J. C. Prasana, and S. Muthu, Spectrochim. Acta, Part A **181**, 153 (2017).
49. T. Koopmans, Physica (Amsterdam, Neth.) **1**, 104 (1934).
50. R. S. Mulliken, J. Chem. Phys. **2**, 782 (1934).
51. J. Murray and K. Sen, *Molecular Electrostatic Potentials: Concepts and Applications* (Elsevier, Amsterdam, 1996).
52. E. Scrocco and J. Tomasi, Adv. Quantum Chem. **11**, 115 (1978).
53. P. G. Sapan, Synthesis, Master's Thesis (Usak Univ., Usak, Turkey, 2018).